Investigation of the dynamics of periodically perturbed counterflow flames

Karin König[*], Ulrich Maas
Institute of Technical Thermodynamics
University of Karlsruhe (TH)
Karlsruhe, Germany

Abstract

The influence of time-dependent periodic perturbations of the flow field and inflow composition on the dynamic behavior of premixed CH_4-air counterflow flames is investigated using detailed chemical kinetics and a detailed transport model. Comparisons between perturbation and flame response, correlation analyses in state space and local time scale analyses based on the method of Intrinsic Low-Dimensional Manifolds (ILDM) are used to characterize the influence of the perturbation onto the flame. Different effects are discussed: For a flow field perturbation, the flame cannot response to the perturbation instantaneously. Nearly no changes in the element composition despite $Le \neq 1$ can be observed. For the perturbed inflow composition, an equalization of the perturbation due to diffusion processes at high frequencies is obtained. For both kinds of perturbation, variations of the species correlations occur that depend on the frequency of the perturbation.

Introduction

In practical combustion systems such as gas turbines, periodical perturbations caused by e.g. acoustical properties of the burner or the system of inlet pipes can yield a loss of efficiency or even the complete breakdown of the turbine. Solving these problems makes it necessary to investigate the influence of time-dependent perturbations onto the complex interaction between physical and chemical processes in combustion. As simulations of flames with complex geometries including detailed chemistry are computationally expensive or even prohibitive, it is also an important question, whether perturbed combustion systems can be described using reduced mechanisms such as Intrinsic Low-Dimensional Manifolds (ILDMs) [1, 2] in order to minimize the computational effort. Some investigations concerning the effects of flow field respectively inflow composition perturbations have already been performed. Stahl [3] investigates the flame front behavior of a lean CH_4-air flame using a time–dependent strain rate as perturbation and looks e.g. at the amplitude of the flame response and at the time delay between perturbation and flame response over frequency. H_2–air counterflow flames subject to periodical perturbations are treated in [4]. In [5], burner-stabilized laminar premixed CH_4-air flames subject to temporal variations of the equivalence ratio are analysed in view of flame temperature and NO_x–emission. In this paper, we analyse both the influence of periodical perturbations of the flow field as well as the inflow composition (identical to a variation of the mixture equivalence ratio) for different perturbation frequencies and amplitudes. We examine the time scales of the system to get an idea whether there is a major influence of the perturbations onto the chemical kinetics and whether it is possible to use the ILDM-method to reduce the chemical kinetics in systems subject to time–dependent perturbations.

Specific Objectives

This paper analyses the response of a premixed CH_4–air counterflow flame to temporally periodical perturbations of the flow field or the inflow composition in view of a detailed understanding of the coupling between physical and chemical processes in perturbed combustion systems. Different analyses are used in this context: First, we look at the time delay between perturbation and flame response as well as at the amplitude of the flame response. Second, correlation analyses between different species in state space yield information, whether the chemical kinetics is influenced by the perturbation. And third, the ILDM–method [1, 2] is used to analyse the local time scales within the system to gain further knowledge about the chemical kinetics in perturbed systems. These analyses are performed for different perturbation frequencies and amplitudes.

Computational method

The effects of time–dependent periodical perturbations onto a flame are analysed by performing laminar one–dimensional calculations for symmetrical premixed strained CH_4–air counterflow flames. A boundary–layer–approximation is used to describe the counterflow configuration as a one–dimensional system [3] and the resulting conservation equations in one dimension are solved using a time–accurate instationary approach [6]. To allow the simulation of superimposed temporally changing flow fields and inflow compositions, adequate time–dependent boundary conditions are implemented for strain and inflow composition. Strain is represented by the tangential pressure gradient $J = -(1/\mathrm{r}) \cdot \partial \mathrm{p}/\partial \mathrm{r}$ with r as spatial coordinate and p as the pressure. J can also be written as $J = -\rho_{\mathrm{ub}}/\mathrm{a}^2$ with ρ_{ub} as density in the unburnt and a as strain rate [3]. A detailed transport model with $Le \neq 1$ and non–equal diffusivities is used.

---

[*] Corresponding author: koenig@itt.mach.uni-karlsruhe.de

Result of the calculations is a vector of thermokinetic state variables at each spatial location of the system, given as $\boldsymbol{\psi}(\boldsymbol{r}) = (h, p, w_1, ..., w_{n_\mathrm{s}})$ with h as the specific enthalpy, p as pressure and w_i as the mass fractions of the n_s species in the system. Time scale analyses based on local eigenvalue analyses according to the ILDM–method [1, 2] allow to analyse the dynamical behavior of the chemical kinetics. The equations for this analysis can be found in [7].

Results and discussion

Perturbation of the flow field

To simulate a perturbation of the flow field, a time–dependent sinusoidal boundary condition was imposed on the tangential pressure gradient $J = -\rho_\mathrm{ub}/a^2$, corresponding to a variation of strain or a variation of the mixture flow velocity at the burner nozzle. Different mean values for J were chosen to simulate both flames subject to maximum perturbation values whose extinction limit is reached or exceeded and flames for which the maximum perturbation value does not reach the extinction limit (the extinction limit for a stoich. CH_4–air counterflow flame was calculated as $J = -1.68 \cdot 10^6 \mathrm{N/m^4}$). The amplitude of the periodic J–perturbation was chosen to be 50% of the mean value and low and high frequencies (20 Hz – 1000 Hz) were examined. The calculations presented here were performed for a stoichiometric CH_4–air flame assuming a temperature in the unburnt of $298\ \mathrm{K}$ and a pressure of $1\ \mathrm{bar}$. First, we analysed the flame location, defined as the location of the maximum temperature gradient. The flame location shows a periodic profile over time as the perturbation does; it is interesting, that the mean value of the flame location does not correspond to the value of the flame location for a corresponding unperturbed flame (calculated with a strain rate equal to the mean value). A comparison of perturbation and flame location over time displays an increasing time delay between perturbation and flame response and a decreasing amplitude of the flame response with increasing frequency. Both effects show, that the flame is not able to follow the perturbation instantaneously. The higher the perturbation frequencies get, the more the flame reacts to a mean value, but not to the momentary value of the perturbation. These effects were also described by [3]. Both the increasing time delay and the decreasing amplitude of the flame response are effects showing a continuous change with increasing frequency, not a sudden change at a special frequency. If the mean value of J is chosen such that the maximum perturbation value is above the extinction limit, an interesting effect is observed: The flame quenches for low frequencies, whereas it burns for high frequencies. This, again, shows the inability of the flame to follow the perturbation for high frequencies - it only reacts to a mean value. Thus the flame is able to sustain maximum perturbation values beyond the extinction limits for high frequencies. To get an idea about the effects of the time-dependent perturbation onto the chemical kinetics, correlations between different species are analysed using 2–dimensional projections of the state space. Figure 1 shows the profiles of some species for two different perturbation frequencies plotted against CO_2, which is an adequate coordinate for the reaction progress [7]. It can be seen from figure 1, that the different strain values caused by the periodic perturbation give rise to different curves in state space (this corresponds to results in [7], where flames were calculated using different strain rates), each belonging to a correlation between the two species for one momentary strain value. For the low frequency a noticeable variance occurs in the correlations (flame reacts to each momentary value of the pertubation, see above). For the high frequency, the correlation curves are bunched and nearly no variance can be seen (due to the incapability of the flame to follow the perturbation instantaneously at high frequencies; see above). From these results of the species correlation analyses it can be stated, that the chemical kinetics is nearly unaffected by perturbations with high frequencies as the flame is too slow to adjust to the rapidly varying flow field. A description of the bunched curves at high frequencies with one– or at least very low–dimensional correlations is possible. Lower frequencies have an influence on the chemical kinetics. Despite that, describing the chemical kinetics using low–dimensional reaction schemes based on only a few chemical time scales appears to be possible for all frequencies. The question arises, how many dimensions are needed, respectively how many time scales can be de-

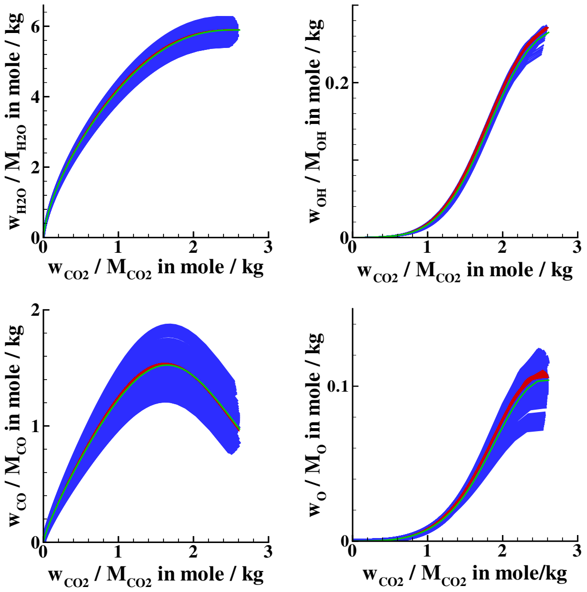

Figure 1: Projections of species into two–dimensional subspaces of the state space; one–dimensional laminar premixed stoichiometric stretched CH_4–air counterflow flame; perturbation of tangential pressure gradient J with $J_\mathrm{mid} = -0.8 \cdot 10^6\ \mathrm{N/m^4}$ and $J_\mathrm{max} = -0.4 \cdot 10^6\ \mathrm{N/m^4}$, 20 Hz (blue) and 1000 Hz (red); detailed transport model; shown are five full periods of the perturbation. Green line: stationary solution for the corresponding unperturbed flame with $J = -0.8 \cdot 10^6\ \mathrm{N/m^4}$.

coupled locally from the perturbed system to gain ILDMs which reduce the computational effort in flame calculations without loosing too much accuracy. Local time scale analyses were peformed to find an answer to this question. Calculation of the time scales used the same algorithm that was used in [7] and some of the results are presented in the following. One important number that is discussed here is the number of relaxed modes, which is the number of processes that can locally be decoupled from the system. The maximum number of relaxed modes for the CH_4–system would be 30, corresponding to the number of reactive variables in the system. The number of relaxed modes gives the necessary dimension of an ILDM to describe the system without exceeding a defined local relative error between detailed and reduced (ILDM) solution. We chose a maximum local error of 5% to show that it is possible to obtain an arbitrary accuracy using the local adaption of the ILDM-dimension; it should be noted that this small error is in effect for all species including minority species and must not be chosen so small for minority species in practical ILDM–calculations. The dimension m of the manifold can be calculated as the difference between the number of reactive variables minus the number of relaxed modes (here $m = 30 - n_{\text{rel}}$). Figure 2 shows the number of relaxed modes for a flame subject to a sinusoidal perturbation of the flow field at a low frequency. The low frequency was chosen, because the species correlations suggest a larger influence of the perturbation onto the chemical kinetics at low frequencies. Results are shown for three different time steps chosen such that the flame is subject to the minimum, maximum and mean perturbation at these time steps. The number of relaxed modes does not differ considerably for the small values of the specific mass fraction of CO_2. More noticeable differences arise for the minimum perturbation value: For the same value of $\mathrm{w}_{\mathrm{CO}_2}/\mathrm{M}_{\mathrm{CO}_2}$, the number of relaxed modes is smaller for the minimum perturbation value as it is for maximum and mean value. The generally small number of relaxed modes can be explained by the chosen small local error for all species (exceeding the error for minority species yields a higher number of relaxed modes) and by the $\mathrm{w}_{\mathrm{CO}_2}/\mathrm{M}_{\mathrm{CO}_2}$–values far away from chemical equilibrium. If the number of relaxed modes is known, it is interesting to see, how the reduced results for that number of relaxed modes look like and how they match with the detailed results. Therefore, figure 3 shows specific mass fractions of different species plotted versus the specific mass fraction of CO_2 for $t = 0.2125$ s, calculated for the detailed and the reduced mechanism which is given by a m-dimensional manifold. The dimension was calculated such that all species have a local error smaller than 5% (corresponding to the number of relaxed modes in figure 2). In each case the lines show the detailed solution, the symbols give the values of the reduced mechanism. As one can see, the reduced solution provides a good approximation for the detailed results. Therefore it is possible to use ILDMs to describe the perturbed systems. Another interesting and important result can be found from the analyses when looking at the element composition. One might expect a changing element composition, as we did not assume $Le = 1$ in the calculations. Contrary to this expectation, figure 4 shows, that there is nearly no change in the element composition with time for given values of CO_2.

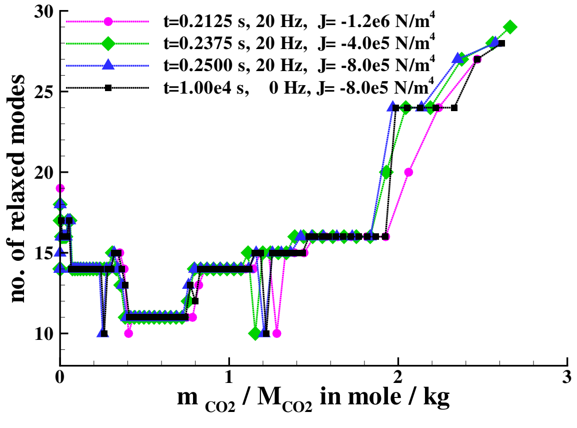

Figure 2: Number of relaxed modes for 3 different time steps; one–dimensional laminar premixed stoichiometric stretched CH_4–air counterflow flame; perturbation of tangential pressure gradient J with $J_{\text{mid}} = -0.8 \cdot 10^6\ \mathrm{N/m^4}$ and $J_{\text{max}} = -0.4 \cdot 10^6\ \mathrm{N/m^4}$, 20 Hz; detailed transport model. Black line: number of relaxed modes for the stationary solution of the corresponding unperturbed flame with $J = -0.8 \cdot 10^6\ \mathrm{N/m^4}$.

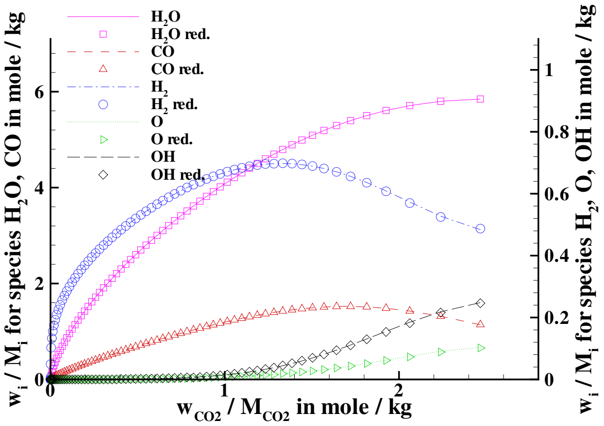

Figure 3: Detailed (lines) and reduced solution (symbols) for different species; one–dimensional laminar premixed stoichiometric stretched CH_4–air counterflow flame; perturbation of tangential pressure gradient J with $J_{\text{mid}} = -0.8 \cdot 10^6\ \mathrm{N/m^4}$ and $J_{\text{max}} = -0.4 \cdot 10^6\ \mathrm{N/m^4}$, 20 Hz; detailed transport model. Reduced mechanism calculated based on a maximum local error of 5%.

Perturbation of the inflow composition

The influence of perturbations of the inflow composition is examined by performing calculations with a time-dependent sinusoidal boundary condition for the CH_4–mass fraction, corresponding to a temporally change of the equivalence ratio. A stoichiometric mixture was con-

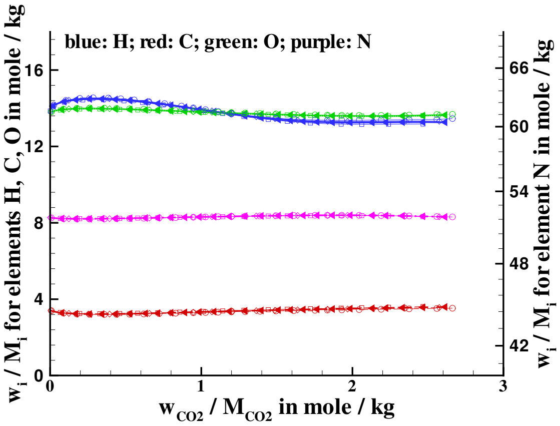

Figure 4: Element composition at three different time steps; one–dimensional laminar premixed stoichiometric stretched CH_4–air counterflow flame, perturbation of tangential pressure gradient J with $J_{\mathrm{mid}}= -0.8 \cdot 10^6\ \mathrm{N/m^4}$ and $J_{\mathrm{max}}= -0.4 \cdot 10^6\ \mathrm{N/m^4}$, 20 Hz (unfilled symbols); detailed transport model. Also shown is the element composition for a corresponding unperturbed flame with $J= -0.8 \cdot 10^6\ \mathrm{N/m^4}$ (filled symbols).

sidered as mean value, different amplitudes (5%, 10% and 30% of the mean value) and frequencies (20 Hz to 1000 Hz) were investigated. The tangential pressure gradient was chosen well below the quenching limit ($J= -0.8 \cdot 10^6\ \mathrm{N/m^4}$). We assumed 298 K as temperature in the unburnt and a pressure of 1 bar. As before for the perturbed flow field, flame quenching can be observed for large values of the perturbation amplitude and low frequencies. Large amplitudes yield temporarily rich respectively lean mixtures with low extinction limits. These extinction limits are exceeded by the chosen values of the strain rate. Because the flame can follow the perturbation instantaneously and therefore reacts to all momentary values, it quenches due to the exceeded extinction limit. At low frequencies, considerable variances in the species correlations are observed. Calculations with high frequencies do not show flame quenching and they also do not show a variance in the species correlations. Explanation for this different behavior at low and high frequencies can be found when looking at figure 5 where the CH_4–perturbation is shown over time and radius. For the low frequency, the perturbation reaches the flame zone (around 0.005 and 0.007 m in the shown example) without a considerable loss of its amplitude. A very different behavior can be seen for the high frequency: During the movement towards the flame zone, the perturbation of the CH_4–mass fraction looses amplitude until the perturbation is completely leveled to a mean value. In the flame zone (which is around 0.0068 m in the shown example), the whole sinusoidal profile of the perturbation has vanished. There are two competing processes: The propagation of the perturbation into the flame zone and the diffusion processes which tend to compensate the perturbation. One can state, that the perturbation of the mass fraction of CH_4 at different frequencies can be compared to the propagation of waves subject to damping effects. In this case of a perturbed flame, the damping effects are caused by diffusion and increase with increasing frequency. The reason for the frequency dependence are different wavelengths caused by different frequencies: At low frequencies, the wavelengths of the perturbations are bigger and those are less subject to dissipation compared to the small wavelenghts at high frequencies. This phenomenon is of practical importance, e.g. for experiments investigating the influence of perturbations, where one has to take care that the perturbation is able to reach the flame. Also, perturbation influences in practical systems might be neglected for high frequencies due to the impossibility for the perturbation to reach the flame. Time scale analyses were performed

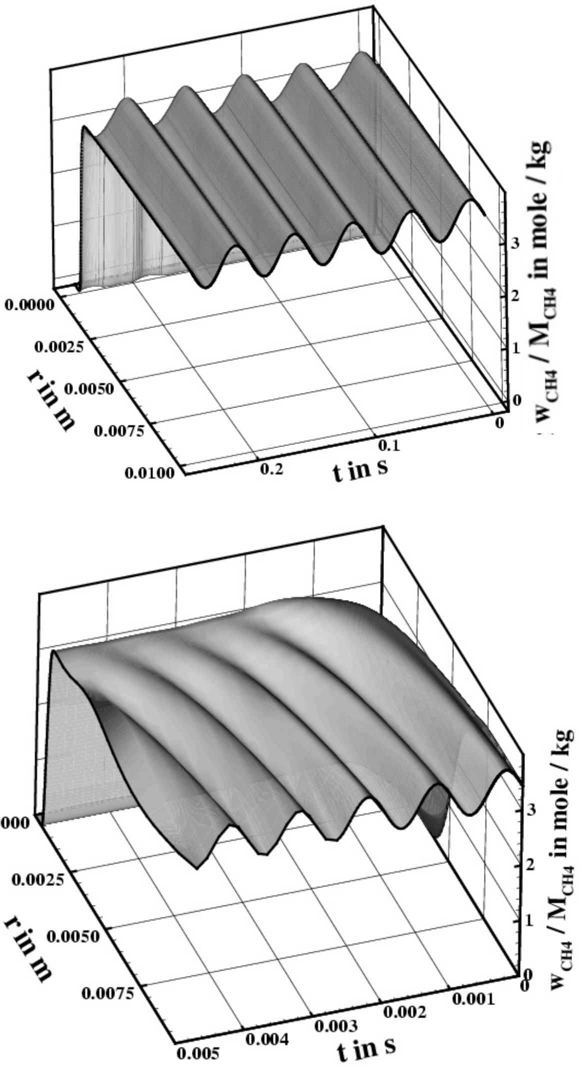

Figure 5: One–dimensional laminar premixed stretched CH_4–air counterflow flame; perturbation of the CH_4–mass fraction; mean value of CH_4 corresponds to stoichiometric mixture, amplitude 10% of mean value, frequency 20 Hz (top) and 1000 Hz (bottom); $J= -0.8 \cdot 10^6\ \mathrm{N/m^4}$; detailed transport model; shown are five full periods of the perturbation.

(see before) and show that the chemical kinetics can be described by nearly the same number of relaxed modes, independent on the momentary value of the perturbation. Comparisons between detailed and a reduced description were performed; they are not discussed here, as they provide the same good results that were discussed in context of the flow field perturbation. Figure 6 shows the element composition at three time steps (minimum, maximum and mean perturbation value) for the perturbed flame and for the stationary solution of the corresponding unperturbed flame. As one can see, the element composition changes for every time step respectively for every current perturbation value. On the other hand the shape of the curves is always similar which indicates correlations of the element mass fractions caused by the properties of the diffusion process.

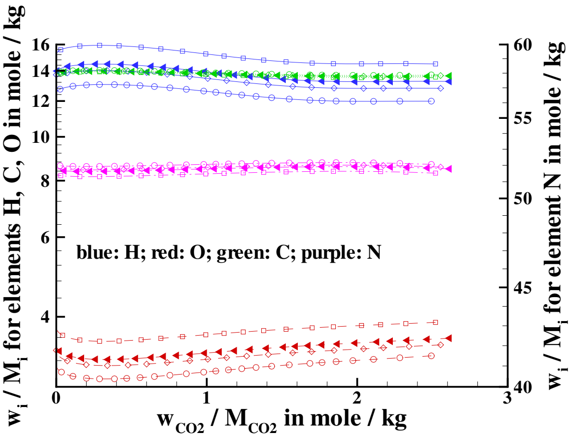

Figure 6: Element composition for 3 different time steps; perturbed one–dimensional laminar premixed stretched CH_4–air counterflow flame with a mean value of CH_4 corresponding to stoichiometric mixture, amplitude 10% of the mean value, frequency 20 Hz (unfilled symbols). Also shown is the element composition for the corresponding stoichiometric unperturbed counterflow flame (filled symbols). For both flames: $J = -0.8 \cdot 10^6$ $\mathrm{N/m^4}$.

Conclusions

In this paper, we analysed the influence of time–dependent periodical perturbations of the flow field and the inflow composition on premixed stretched CH_4–air counterflow flames using detailed chemistry and a detailed transport model. Periodical perturbations of the flow field are represented by a temporally sinusoidal change of the tangential pressure gradient; different perturbation frequencies were investigated for a stoichiometric CH_4–air counterflow flame. It is shown, that the flame cannot response to the perturbation instantaneously. At high frequencies, the flame responses to a mean value only. An important result is that the varying strain rates yield a nearly constant local element composition in composition space, even though the Lewis-number was $\neq 1$. From species correlation analyses and time scale analyses it can be seen that it is possible to find lower–dimensional descriptions of the perturbed systems at all frequencies with the necessary dimension decreasing with increasing frequency. Further calculations were performed to analyse the influence of a temporally sinusoidal variation of the inflow composition represented by a changing CH_4–mass fraction. Different perturbation amplitudes and different frequencies were investigated assuming a strain rate well below the quenching limit. Flame quenching occurs for high perturbation amplitudes and low frequencies due to the combination of inflow composition with its characteristic extinction limit and the chosen value of the strain rate. At high frequencies, the perturbation of the inflow composition does not reach the flame zone, as it is compensated by diffusion processes before reaching the flame. A description of systems with perturbed inflow composition with ILDMs is possible.

Acknowledgements

The authors thank the Deutsche Forschungsgemeinschaft and the German Israeli Foundation for financial support.

References

[1] U. Maas, S. B. Pope, *Combust. Flame* 88 (1992) 239-264.

[2] U. Maas, S. B. Pope, *Proc. Combust. Inst.* 24 (1992) 103-112.

[3] G. Stahl, J. Warnatz, *Combust. Flame* 85 (1991) 285-299.

[4] N. Darabiha, *Comb. Sci. and Techn.* 86 (1992) 163-181.

[5] N. Darabiha, S. Candel, D. A. Wirth, J. R. Mahan, *Comb. Sci. and Techn.* 113-114 (1996) 35-47.

[6] U. Maas, J. Warnatz, *Combust. Flame* 7a (1988) 53-69.

[7] D. Schmidt, T. Blasenbrey, U. Maas, *Combust. Th. Mod.* 2 (1998) 135-152.